Solution processed nickel oxide anodes for organic photovoltaic devices

Bestoon Mustafa, Jonathan Griffin, Abdullah S. Alsulami, David G. Lidzey, and Alastair R. Buckley

Citation: Applied Physics Letters **104**, 063302 (2014); doi: 10.1063/1.4865090
View online: http://dx.doi.org/10.1063/1.4865090
View Table of Contents: http://scitation.aip.org/content/aip/journal/apl/104/6?ver=pdfcov
Published by the AIP Publishing

Solution processed nickel oxide anodes for organic photovoltaic devices

Bestoon Mustafa, Jonathan Griffin, Abdullah S. Alsulami, David G. Lidzey, and Alastair R. Buckley[a)]
Department of Physics and Astronomy, Hicks Building, Hounsfield Road, University of Sheffield, Sheffield S3 7RH, United Kingdom

(Received 18 December 2013; accepted 23 January 2014; published online 11 February 2014)

Nickel oxide thin films have been prepared from a nickel acetylacetonate (Ni(acac)) precursor for use in bulk heterojunction organic photovoltaic devices. The conversion of Ni(acac) to NiO_x has been investigated. Oxygen plasma treatment of the NiO layer after annealing at 400 °C affords solar cell efficiencies of 5.2%. Photoelectron spectroscopy shows that high temperature annealing converts the Ni(acac) to a reduced form of nickel oxide. Additional oxygen plasma treatment further oxidizes the surface layers and deepens the NiO work function from 4.7 eV for the annealed film, to 5.0 eV allowing for efficient hole extraction at the organic interface. [http://dx.doi.org/10.1063/1.4865090]

Silicon, cadmium telluride, and a minority of other solar cell technologies are being adopted in many nations for domestic rooftop, commercial rooftop, and ground mounted power plant electricity generation.[1,2] However photovoltaic (PV) electricity generation still suffers high capital costs.[3] Therefore there is a continued emphasis on research to reduce the financial barrier to PV deployment through the development of cell technologies and fabrication processes that result in substantial cost reductions.[4] One technology group that addresses this is the polymer organic PV cell (OPV) that incorporates a bulk heterojunction (BHJ) donor-acceptor structure.[5,6] These systems have been studied intensively because of advantages that include low production cost, simplicity of fabrication, compatibility with flexible and conformable substrate, and the non-toxicity of the waste left behind after production.[1,7–9] However even with dramatic increases in both the power conversion efficiencies (PCEs) and lifetimes over the past decade, they are still not considered commercially viable.

The workhorse organic bulk heterojunction used in OPVs is a blend of poly(3-hexylthiophene) (P3HT) and [6,6]-phenyl C61-butyric acid methyl ester (PCBM).[10] There are several factors that limit the PCE of P3HT-based devices. The large electronic band gap of P3HT (~2.5 eV) leads to only limited absorption of the solar spectrum[11] and poor energetic alignment of the donor (polymer) and the acceptor (fullerene) limit the open circuit voltage (V_{oc}) to ~0.6 V.[7] The use of newer donor materials such as [poly[N-9″-heptadecanyl-2,7-carbazole-alt-5,5-(4′,7′-di-2-thienyl-2′,1′,3′- benzothiadiazole)]] (PCDTBT) have overcome these limitations with lower bandgap (1.8 eV) and deeper HOMO/LUMO levels of −5.3 eV/−3.5 eV.[12] Devices incorporating PCDTBT and $PC_{70}BM$ obtain PCEs above 7% and internal quantum efficiencies approaching 100% when the optical thickness and electrical properties of devices are optimised.[13–15] PEDOT:PSS (polyethylene di-oxythiophene polystyrene sulphonate) is used as a standard anode interface in OPVs to increase the extraction of holes.[16–19] However PEDOT:PSS exhibits several undesirable degradation mechanisms. PSS leads to the decomposition of In_2O_3 in indium tin oxide (ITO) due to its high acidity and due to the deep HOMO level of PCDTBT and similar donor materials, energy barriers to charge extraction can form.[19–22] To overcome these issues metal oxides such as MoO_3,[23] WO_3,[24] V_2O_5,[25] and NiO (Refs. 10 and 19) have recently been used with promising results.

In this work we show that it is possible to solution process nickel oxide from a nickel acetylacetonate precursor and obtain a power conversion efficiency of 5.2%. This is achieved by the use of post deposition thermal annealing and oxygen plasma treatment. We show that annealing leads to the thermal decomposition of the acetylacetonate precursor causing a deepening of the work function and a reduction in oxidation state. Post annealing oxygen plasma treatment further reduces the work function by oxidizing the surface layer of the sample that facilitates charge extraction at the organic interface.

To prepare the OPV devices, nickel acetylacetonate (99.99%) was purchased from Sigma Aldrich and was dissolved in toluene at a concentration of 15 mg/ml. Organic photovoltaic devices were fabricated on ITO coated glass substrates. The substrates were cleaned in de-ionized water and Hellmanex by sonicating for 10 min at 75 °C. After sonication, they were washed with the de-ionized water. They were then placed in iso-propanol and sonicated for 10 min at 75 °C. Finally, they were dried with nitrogen gas. Thin films (~3 nm) of nickel acetylacetonate were deposited via spin coating onto cleaned ITO substrates and were either annealed at between 100 °C and 400 °C for 30 min in air, or left un-annealed. O_2 plasma treatment of NiO thin films was carried out in a 10 cm diameter barrel reactor for 1, 2, and 3 min at varying pressures and powers. The active layer was prepared by mixing solutions of PCDTBT and $PC_{70}BM$ at a weight ratio of 1:4 in chlorobenzene with an overall concentration of 20 mg/ml. The PCDTBT:$PC_{70}BM$ solution then was spin coated at 700 rpm in a glove box. Samples were loaded into a vacuum chamber and pumped down to a base pressure of ($<10^{-6}$ mbar). A calcium (3 nm) then aluminium (100 nm) double layer cathode was deposited via thermal

a)alastair.buckley@sheffield.ac.uk

evaporation. After deposition of the cathode, devices were encapsulated using an inert UV curable epoxy and a glass cover slide. Each device had an area of approximately 4.5 mm^2 as defined by a shadow mask and were measured under ambient conditions using a Keithley 2400 source meter and a Newport 92251A-1000 AM1.5 solar simulator. An NREL calibrated silicon diode was used to calibrate the power output at 100 mW/cm^2. XPS and UPS were carried out using a Kratos Ultra AXIS photoelectron spectrometer. XPS measurements were taken using the Al Kα emission line (1486 eV), a band pass energy of 10 eV, a step size of 0.025 eV, and a dwell time of 250 ms. UPS measurements were taken using the He (I) emission line (21.2 eV), a band pass energy of 10 eV, a step size of 0.025 eV, and a dwell time of 250 ms.

Figure 1 shows the current density-voltage characteristics of the devices that use a nickel acetylacetonate (Ni(acac)) film as the hole extraction layer. The effects of thermal annealing and the post annealing O_2 plasma treatments of Ni(acac) film are shown. In Figure 1(a), devices incorporating as cast films of Ni(acac) and Ni(acac) films that have been thermally annealed at temperatures ranging between 200 °C and 300 °C are shown. Devices with an as cast Ni(acac) layer show the lowest

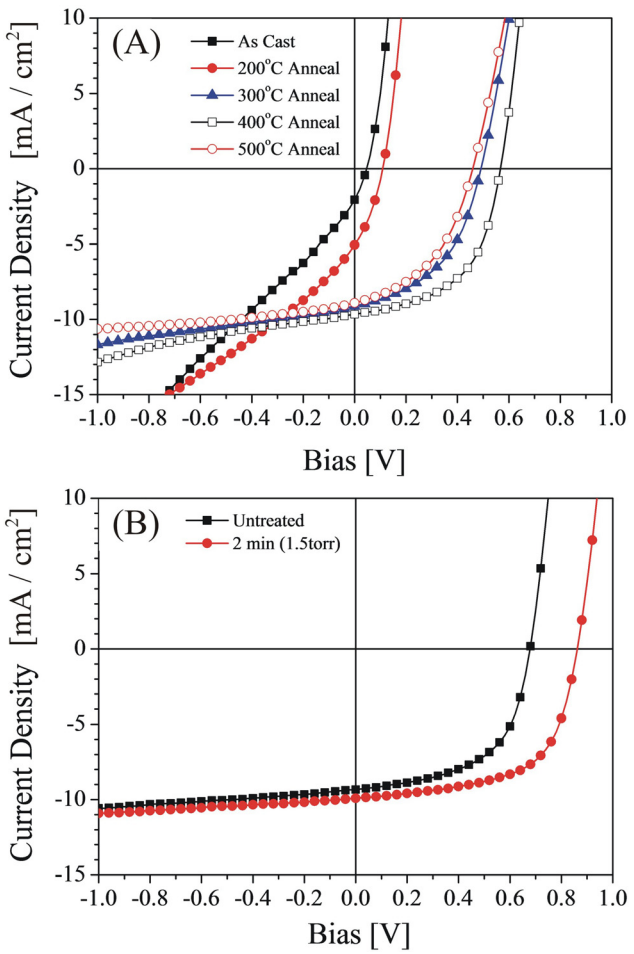

FIG. 1. The current density-voltage characteristics of organic photovoltaics. (a) is for thermally annealed films (filled squares for the as cast Ni(acac), filled circles for 200 °C anneal, filled triangles for 300 °C, open squares for 400 °C, and open circles for 500 °C anneal) and (b) is for films with (filled circles) and without (filled squares) oxygen plasma treatment post annealing at 400 °C.

performance. However, annealing at higher temperatures leads to an increase in device performance up until a maximum value of 400 °C. The J-V curves show a dramatic increase in the shunt resistance of the devices as the Ni(acac) film is annealed beyond a critical point, as indicated by the reduced gradient in the reverse bias region. The origin of this dramatic shift is likely due to the thermal decomposition of the Ni(acac) layer leading to the formation of NiO. For non-annealed NiO, the highest PCE, fill factor (FF), short circuit current density (J_{sc}), and open circuit voltage (V_{OC}) were 0.06%, 31.5%, −2.91 mA/cm, and 0.06 V, respectively. Annealing of NiO from 100–400 °C showed an increase in device performances, continuously with increasing the annealing temperature. For example, PCE, FF, V_{oc}, and J_{sc} were increased from 0.1%, 32.8% (at 100 °C) to 3.5%, 56.2% (at 400 °C) respectively. It was found that optimum annealing temperature for Ni(acac) films was between 350 °C and 400 °C (Table I).

Ni(acac) thin films were also treated using an O_2-plasma following thermal annealing at 400 °C. Varying oxygen pressures and treatment times were used. Figure 1(b) shows devices using films that were not treated with an O_2-plasma against films that were treated at the optimal pressure and time. For films treated at 1.5 Torr for 2 min it is observed that there is an increase in the V_{OC} of approximately 0.19 eV and in addition a small increase in the J_{sc} of 0.6 mA/cm^2 occurs. The device efficiency parameters are summarised in Table II for the various pressures and times used. The enhancement in power conversion efficiency for all plasma treated device is driven by the increase in V_{oc} of over 25% and slight increases in the J_{SC} and FF. These changes are likely caused by the oxidation of the surface layer of the NiO film, as the results indicate that both the V_{OC} and FF are independent of the time and pressure that the films are treated for. XPS of the C1s spectra (not shown) indicate that removal of residual organic content from the surface is not the cause as the thermal annealing leads to the removal of this material. The enhancement in efficiency however could be due to further oxidation of the surface layer leading to a deepening of the work function. Both of these would lead to reduced charge carrier recombination and contact resistances.[26]

Ultraviolet photoelectron spectroscopy is a useful tool for probing the work function (Φ), interfacial dipole, and ionization energy (IE) of films.[27,28] Figure 2 shows the secondary electron cut off and the valence band region of He(I) UPS spectra of Ni(acac) films that have undergone thermal annealing and post annealing O_2-plasma treatment. Figure 2(a) shows the UPS spectra of Ni(acac) as deposited and for

TABLE I. Performance of OPV test devices containing nickel oxide anode buffer layer annealed at different temperatures. Test conditions were at 25 °C under AM1.5 irradiance.

Annealing temperature [°C]	FF [%]	PCE [%]	J_{sc} [mA/cm^2]	V_{oc} [V]
Non-annealed	31.5	0.06	−2.91	0.06
100	32.8	0.1	−3.39	0.097
300	50.4	2.42	−9.2	0.52
400	56.22	3.55	−9.33	0.67

TABLE II. Performance of OPV test devices containing nickel oxide anode buffer layer annealed at 400 °C and exposed to O_2 plasma for different times and pressures. Test conditions were at 25 °C under AM1.5 irradiance.

	Baseline	O_2 plasma treatment					
Device performance parameters	400 °C anneal	0.5 mbar 1 min	0.5 mbar 2 min	0.5 mbar 3 min	1.5 mbar 2 min	1.5 mbar 2 min	1.5 mbar 3 min
V_{OC} [V]	0.67	0.86	0.86	0.86	0.84	0.86	0.86
Jsc [mA/cm^2]	−9.3	−8.9	−9.5	−9.6	−9.5	−9.9	−9.6
FF [%]	56.2	61.1	60.5	59.8	59.9	60.8	59.8
PCE [%]	3.5	4.68	5.0	5.0	4.84	5.2	5.0

films annealed at 250 °C and 500 °C. The work function for as deposited films is determined to be −3.7 eV and upon annealing this value shifts to −4.7 eV. In addition the valence states appear closer to the Fermi level however the states do not extend to the Fermi level indicating that the films are still semiconducting in nature. This deepening of the work function is likely to lead to more favourable energy level alignment between the HOMO of PCDTBT. In addition, XPS measurements of the C1s peak (not shown in manuscript) indicate that the thermal decomposition of the Ni(acac) occurs to completion at 300 °C. This will remove any trap states that are present on the ligand of the Ni(acac) precursor. These combination of would explain the observed changes within the device results. Figure 2(b) shows Ni(acac) thin films with and without O_2-plasma treatment (after annealing at 400 °C). The work function shows a further deepening by −0.3 eV to −5 eV upon treatment of the films. This deepening of work function and the deepening of the valence band of the material in comparison to the Fermi level is typical of highly oxidized hole extracting metal oxides such as molybdenum oxide.[29] This suggests that the annealed precursor is a slightly reduced form of NiO and that O_2-Plasma treatment leads to the oxidation of the surface layer at the anode/organic interface.

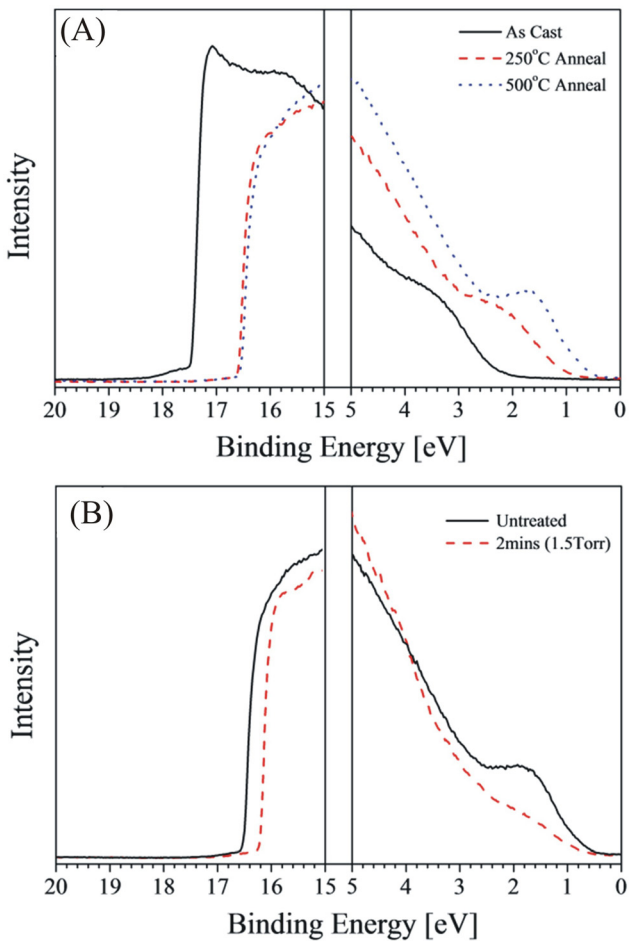

FIG. 2. UPS measurements for Ni(acac) films deposited onto ITO. (a) Shows films as-deposited (solid line) and with post deposition annealing at 250 °C (dashed line) and 500 °C (dotted line), (b) shows films with (solid line) or without (dashed line) oxygen plasma treatment after post deposition annealing at 400 °C.

XPS results for Ni(acac) films with and without post annealing O_2-plasma treatment are shown in Figure 3. The O 1s spectra is shown in Figure 3(a) and contains a main peak at 529.4 eV and originates from oxygen atoms bound to nickel within the nickel oxide film.[26] A secondary peak is also present at a higher binding energy of 531.0 eV and is attributed to hydroxide ions that are present in adsorbed water. A final diffuse peak manifests itself as tail states in the spectra and this is due to oxygen in adsorbed water on the surface. It can be seen that for the treated films both the relative intensity of the hydroxide and the water peak increase in relation to the oxygen present within the NiO lattice. This indicates that an increased amount of water is present at the film surface. Previous studies on metal oxides show that water adsorption relates strongly to film density.[30,31] Since the density of the fully oxidised NiO film is less than that of metallic Nickel it is likely that highly oxidized surface layers would lead to increased water adsorption. The Ni 2p peaks shown in Figure 3(b) consists of several doublet peaks separated by approximately 18 eV, the ratio of the area of these doublet peaks is 1:2. The spectrum consists of 3 sets of doublet peaks with the larger, low energy peaks being

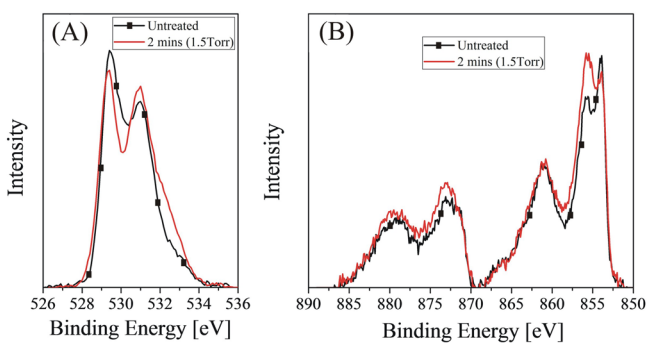

FIG. 3. XPS spectra of Ni(acac) films with (solid line) and without (solid line with squares) post annealing O_2-plasma treatment. (a) Shows the O 1s spectra and (b) shows the Ni 2p spectra.

found at, for metallic nickel (Ni^0), 853.9 eV, for oxidized nickel (Ni^{+1}), at 854.8 eV, and for doubly oxidized nickel peak (Ni^{+2}), at 856.4 eV. The relative peak intensities depend on both the average oxidation state of the film between the surface and the penetration depth of the XPS instrument. However it can be observed that upon treating the films with an O_2-Plasma that the total amount of Ni^0 is reduced in relation to the other two peaks. This decrease is accompanied by an increase in the Ni^{+1} oxidation state. This indicates that the plasma treatment converts the metallic Ni^0 states to Ni^{+1} states at the surface.

The combination of XPS, UPS, and device data suggest that as the Ni(acac) precursor is heated beyond a critical temperature the conversion of the precursor to NiO occurs. The high temperatures required to do this however lead to the reduction in oxidation state of the NiO to a sub oxide NiO_{1-x}. However these metallic states at the surface of the film cause a reduction in the depth of the work function in comparison to that of fully oxidized Nickel. Upon treatment with an O_2-plasma further metallic surface states are oxidized. The deep work function of this oxidized interface allows for the efficient extraction of holes due to a reduced energy barrier in comparison to that of the NiO_{1-x} film. For metal oxide precursors that require high temperature annealing the use of an O_2-plasma post-treatment could be an effective way of increasing device performance by reducing any potential interfacial barriers that may occur due to the presence of metallic states. It is possible that the change in surface electronic structure on annealing and/or plasma treatment has a knock on effect on the morphology of the bulk heterojunction. Such an effect could be correlated with changes due to the energetic alignment at the anode interface. However we can be fairly sure that this morphology effect is negligible compared with the impact anode energy alignment in the case of plasma treated versus untreated since the short circuit current of the devices without plasma treatment ($-9.3\,mA/cm^2$) are within the experimental range of the plasma treated devices (-8.9 to $-9.9\,mA/cm^2$) indicating there has been no significant change in the mobility of the bulk polymer layer between these devices. For unannealed Ni(acac) devices we cannot be so sure that morphology changes are not present, however, given the severity of the open circuit voltage reduction for unannealed films (<0.1 V versus >0.8 V for annealed devices) we are confident they are minor compared to the changes in performance caused by the influence of the interface electronic structure.

In conclusion, the solution processing of thin films of nickel oxides from a Ni(acac) precursor for use in organic photovoltaics have been studied. This work has shown that the performance of OPVs containing NiO films deposited from these precursors depend strongly upon post deposition treatment. Thermal annealing at temperatures of 300 °C and above is needed to drive the conversion of the precursor into the metal oxide leading to an increase in PCEs from 0.06% to 3.5%; this has been attributed to the deeper work function of nickel oxide, −4.7 eV compared to −3.7 eV for the precursor, and reduced recombination at the organic interface. Treatment of annealed films with an oxygen plasma leads to further increases in efficiency with a reported peak PCE of 5.2%. This is attributed to the oxidation of reduced states at the films surface that appear due to the high temperature thermal annealing needed to convert the precursor. This oxidation leads to a further deepening of the work function to −5.0 eV leading to a reduced extraction barrier at the organic interface.

This work was undertaken by the Electronic and Photonic Molecular Materials research group at the University of Sheffield and was supported financially by the UK Engineering and Physical Sciences Research Council (EPSRC) under Grant Nos. EP/I032541/1 (Solar Energy in Future Societies), EP/I028641/1 (Polymer/fullerene photovoltaic devices: new materials and innovative processes for high-volume manufacture), and EP/J017361/1 (Supergen Supersolar network).

[1]A. Shah, P. Torres, R. Tscharner, N. Wyrsch, and H. Keppner, Science **285**, 692–698 (1999).
[2]M. A. Green, K. Emery, Y. Hishikawa, W. Warta, and E. D. Dunlop, Prog. Photovoltaics **20**, 12–20 (2011).
[3]A. C. Mayer, S. R. Scully, B. E. Hardin, M. W. Rowell, and M. D. McGehee, Mater. Today **10**, 28–33 (2007).
[4]K. L. Chopra, P. D. Paulson, and V. Dutta, Prog. Photovoltaics **12**, 69–92 (2004).
[5]Y. Liang, Z. Xu, J. Xia, S. T. Tsai, Y. Wu, G. Li, C. Ray, and L. Yu, Adv. Mater. **22**, E135–E138 (2010).
[6]M. C. Scharber, D. Mühlbacher, M. Koppe, P. Denk, C. Waldauf, A. J. Heeger, and C. J. Brabec, Adv. Mater. **18**, 789–794 (2006).
[7]B. Kim, H. R. Yeom, M. H. Yun, J. Y. Kim, and C. Yang, Macromolecules **45**, 8658–8664 (2012).
[8]J. S. Moon, J. Jo, and A. J. Heeger, Adv. Energy Mater. **2**, 304–308 (2012).
[9]S. Günes, H. Neugebauer, and N. S. Sariciftci, Chem. Rev. **107**, 1324–1338 (2007).
[10]M. D. Irwin, D. B. Buchholz, A. W. Hains, R. P. H. Chang, and T. J. Marks, Proc. Natl. Acad. Sci. **105**, 2783–2787 (2008).
[11]Z. L. Guan, J. B. Kim, H. Wang, C. Jaye, D. A. Fischer, Y. L. Loo, and A. Kahn, Org. Electron. **11**, 1779–1785 (2010).
[12]E. L. Ratcliff, J. Meyer, K. X. Steirer, N. R. Armstrong, D. Olson, and A. Kahn, Org. Electron. **13**, 744–749 (2012).
[13]S. H. Park, A. Roy, S. Beaupré, S. Cho, N. Coates, J. S. Moon, D. Moses, M. Leclerc, K. Lee, and A. J. Heeger, Nature Photonics **3**, 297–302 (2009).
[14]Y. Sun, C. J. Takacs, S. R. Cowan, J. H. Seo, X. Gong, A. Roy, and A. J. Heeger, Adv. Mater. **23**, 2226–2230 (2011).
[15]N. Blouin, A. Michaud, and M. Leclerc, Adv. Mater. **19**, 2295–2300 (2007).
[16]R. Steim, F. R. Kogler, and C. J. Brabec, J. Mater. Chem. **20**, 2499–2512 (2010).
[17]Y. Cao, G. Yu, C. Zhang, R. Menon, and A. J. Heeger, Synth. Met. **87**, 171–174 (1997).
[18]K. X. Steirer, P. F. Ndione, N. E. Widjonarko, M. T. Lloyd, J. Meyer, E. L. Ratcliff, A. Kahn, N. R. Armstrong, C. J. Curtis, D. S. Ginley, J. J. Berry, and D. C. Olson, Adv. Energy Mater. **1**, 813–820 (2011).
[19]J. R. Manders, S. W. Tsang, M. J. Hartel, T. H. Lai, S. Chen, C. M. Amb, J. R. Reynolds, and F. So, Adv. Funct. Mater. **23**, 2993–3001 (2013).
[20]J. Kettle, H. Waters, M. Horie, and S. W. Chang, J. Phys. D **45**, 125102 (2012).
[21]T. Y. Chu, S. Alem, P. G. Verly, S. Wakim, J. Lu, Y. Tao, S. Beaupré, M. Leclerc, F. Bélanger, D. Désilets, S. Rodman, D. Waller, and R. Gaudiana, Appl. Phys. Lett. **95**, 063304 (2009).
[22]J. Jung, D. L. Kim, S. H. Oh, and H. J. Kim, Sol. Energy Mater. Sol. Cells **102**, 103–108 (2012).
[23]A. K. Kyaw, X. W. Sun, C. Y. Jiang, G. Q. Lo, D. W. Zhao, and D. L. Kwong, Appl. Phys. Lett. **93**, 221107 (2008).
[24]S. Han, W. S. Shin, M. Seo, D. Gupta, S. J. Moon, and S. Yoo, Org. Electron. **10**, 791–797 (2009).
[25]G. Li, C. W. Chu, V. Shrotriya, J. Huang, and Y. Yang, Appl. Phys. Lett. **88**, 253503 (2006).

[26]E. L. Ratcliff, J. Meyer, K. X. Steirer, A. Garcia, J. J. Berry, D. S. Ginley, D. C. Olson, A. Kahn, and N. R. Armstrong, Chem. Mater. **23**, 4988–5000 (2011).
[27]J. S. Kim, B. Lägel, E. Moons, N. Johansson, I. D. Baikie, W. R. Salaneck, R. H. Friend, and F. Cacialli, Synth. Met. **111**, 311–314 (2000).
[28]D. Cahen and A. Kahn, Adv. Mater. **15**, 271–277 (2003).
[29]M. T. Greiner, M. G. Helander, W. M. Tang, Z. B. Wang, J. Qiu, and Z. H. Lu, Nature Mater. **11**, 76–81 (2012).
[30]E. Bovill, J. Griffin, T. Wang, J. W. Kingsley, H. Yi, A. Iraqi, A. R. Buckley, and D. G. Lidzey, Appl. Phys. Lett. **102**, 183303 (2013).
[31]D. R. Lide, *Handbook of Chemistry and Physics*, 79th ed. (CRC Press, Boca Raton, 1998).